

Orientationally ordered island growth of higher fullerenes on Ag/Si(111)-($\sqrt{3}\times\sqrt{3}$)R30°

M. J. Butcher, J. W. Nolan, M. R. C. Hunt, and P. H. Beton

School of Physics and Astronomy, University of Nottingham, Nottingham, NG7 2RD, United Kingdom

L. Dunsch, P. Kuran, and P. Georgi

IFW Dresden, Group of Electrochemistry and Conducting Polymers, D-01171 Dresden, Germany

T. J. S. Dennis

Department of Chemistry, Queen Mary and Westfield College, University of London, London E1 4NS, United Kingdom

(Received 1 November 2000; revised manuscript received 15 March 2001; published 12 October 2001)

The adsorption of the higher endohedral and empty fullerenes La@C₈₂ and C₈₄ on Ag/Si(111)-($\sqrt{3}\times\sqrt{3}$)R30° has been investigated using ultrahigh-vacuum scanning tunneling microscopy. At low coverage these molecules form single-layer islands with orientational order, a consequence of the commensurability between the intermolecular separation for each species and the surface lattice constant. The preferred adsorption site for the molecules is above an Ag trimer. Several other domains are observed at higher coverage which may be understood using a simple model. Following annealing, domains with a single orientation remain and the possibilities for epitaxial and heteroepitaxial growth are discussed.

DOI: 10.1103/PhysRevB.64.195401

PACS number(s): 68.43.Fg

I. INTRODUCTION

Over the period since C₆₀ was isolated in gram-scale quantities, the adsorption of fullerenes on many different surfaces has been studied.¹ In general, islands are formed in which the growing faces parallel to the substrate surface are hexagonally ordered.²⁻¹² Nucleation at different sites on the surface generally occurs and, with few exceptions,^{8,12} this results in a variation from island to island of the orientation of the principal axes of the adsorbed layers. As a consequence, thick films of fullerenes are polycrystalline and epitaxial growth is not generally possible.

The growth of C₆₀ on Si(111)-(7×7) provides an interesting example of fullerene growth in that domains are formed in which the principal axes display only two orientations.¹⁰ The misorientation of these domains with respect to the underlying silicon substrate is related to the lack of commensurability of the C₆₀ intermolecular separation and the Si lattice constant. On the basis of these results, it has been suggested¹¹ that for a substrate-fullerene combination for which a commensurability between the intermolecular spacing and Si surface lattice constant exists, growth of domains with only one orientation would be expected, leading to the possibility of epitaxial growth.

In this paper we discuss the deposition of higher fullerenes La@C₈₂ and C₈₄ on the Ag/Si(111)-($\sqrt{3}\times\sqrt{3}$)R30° surface. These molecules are chosen for study since their intermolecular separation, which is greater than C₆₀, is commensurate with the silicon lattice. Both these molecules exhibit growth, which leads primarily to the formation of domains with a single orientation, which we show is related to this commensurability. The observation that two fullerenes exhibit growth with the same orientational order leads to the possibility that epitaxy and lattice matched heteroepitaxy may be feasible.

II. EXPERIMENT

The experiments were carried out using (5×3) mm² pieces of Si(111) *p*-type wafer. After transfer into an ultrahigh-vacuum (UHV) system, the samples are outgassed at ~800 °C for 12 h. They are then flash annealed to ~1200 °C for 60 s and allowed to cool to room temperature. This process consistently results in the formation of a clean (7×7) reconstruction. The Ag/Si(111)-($\sqrt{3}\times\sqrt{3}$)R30° surface was prepared by depositing Ag onto the clean Si(111)-7×7 surface while heating the substrate at ~450 °C. Scanning tunneling microscopy (STM) imaging of the surfaces is undertaken at room temperature using electrochemically etched polycrystalline W tips. The tips were cleaned in the UHV system by electron beam heating.

The La@C₈₂ soot was prepared by the Krätschmer arc vaporization method¹³ in a modified form.¹⁴ The soluble soot components were extracted with a Soxhlet by CS₂ and finally dissolved in xylene. The La@C₈₂ was purified using high-performance liquid chromatography (HPLC) separation on a preparative HPLC system (Gilson Abimed) with a Cosmosil Buckyprep column (Nacalai, 25 cm×2 cm) and toluene as a mobile phase (10 ml/min). The injection volume was 5 ml. The temperature of the column was kept at 30.0 °C. For further separation of the single isomeric form, an analytical HPLC (Hewlett Packard series 1050) a Buckyclutcher column (SES, 25 cm×1 cm) was used applying a mixture of toluene/hexane (9/1) as the eluent (2.2 ml/min). The injection volume was 300 μl. The purity of the La@C₈₂ was higher than 95% as determined by mass spectrometry. The La@C₈₂ was sublimed at 510 °C onto the clean Ag/Si(111)-($\sqrt{3}\times\sqrt{3}$)R30° surface, which was held at room temperature, with a rate of 0.1 monolayers (ML)/h (1 ML is equivalent to one hexagonally ordered layer of molecules with an intermolecular separation equal to that observed in the corresponding bulk crystal).

The C₈₄ was prepared by arc burning graphite rods in a

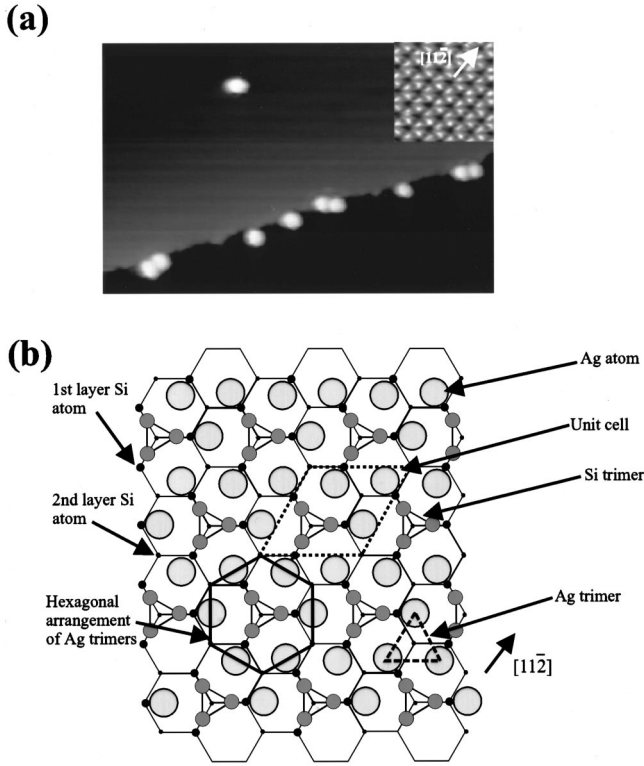


FIG. 1. (a) $35 \times 20 \text{ nm}^2$ STM image of a low coverage of La@C_{82} on $\text{Ag/Si}(111)-(\sqrt{3} \times \sqrt{3})R30^\circ$. Tunneling current is 0.1 nA and bias voltage is -2.8 V . Inset shows a contrast enhanced image of the $\sqrt{3} \times \sqrt{3}$ reconstruction ($3.5 \times 3.5 \text{ nm}^2$). (b) Schematic showing the honeycomb-chain-trimer model for the $\text{Ag/Si}(111)-(\sqrt{3} \times \sqrt{3})R30^\circ$ reconstruction.

The stream followed by isolation and purification (including removal of minor isomers) using HPLC.¹⁵ The charge contained a 2:1 mixture of the two most common isomers, D_2 and D_{2d} , and was sublimed at 455°C at a rate of 0.005 ML/h.

III. RESULTS AND DISCUSSION

A. La-C_{82} island growth

Figure 1(a) shows a typical STM image of a low coverage (0.005 ML) of La@C_{82} molecules adsorbed on the $\text{Ag/Si}(111)-(\sqrt{3} \times \sqrt{3})R30^\circ$ surface. The bright near-circular features are the adsorbed La@C_{82} molecules. As for C_{60} ,¹¹ it can be seen that the molecules are able to diffuse on the surface and become bound at reactive sites where there are unsaturated dangling bonds. These sites are at step edges (running across the image) and defects (note molecule bound at the middle of the terrace). The molecules also become trapped at defects known as out of phase domain boundaries (OPB's). This is discussed in Sec. III B.

Recent STM studies of Y@C_{82} (Ref. 16) and Nd@C_{82} (Ref. 17), on surfaces where diffusion can take place, reveal the presence of pairs and small clusters of molecules at low coverage. These observations are attributed to the permanent dipole moment of the molecules. The image in Fig. 1(a) also shows that some of the La@C_{82} molecules form pairs along

the step edge. Their intermolecular separations are between 1.3 and 1.4 nm. This spacing is significantly larger than the bulk separation of La@C_{82} molecules [1.12 nm (Ref. 18)]. The abundance of these pairs at this coverage is also comparable to that of C_{60} , indicating that for this surface their presence is unrelated to the permanent dipole moment which is expected for La@C_{82} .¹⁹

The inset in Fig. 1(a) shows a contrast enhanced region of the $\text{Ag/Si}(111)-(\sqrt{3} \times \sqrt{3})R30^\circ$ reconstruction. The most commonly accepted model for the surface is the honeycomb-chain-trimer (HCT) structure first proposed by Takahashi *et al.*²⁰ A schematic diagram of the reconstruction is shown in Fig. 1(b). Within the $\sqrt{3} \times \sqrt{3}$ unit cell there are three Ag atoms arranged as a trimer, which is located above a second-layer Si atom. Each of the Ag atoms is involved in bonding to one of the Si trimer atoms so that all of the dangling bonds are saturated. The Ag atoms form a hexagonal ring around the Si trimer, and this is observed in the STM image as the honeycomb structure (the bright and dark regions relate to the hexagonal arrangement of Ag trimers and Si trimers, respectively).

Further deposition of La@C_{82} leads to the formation of small islands that grow out from the reactive sites at the surface. Most importantly, and unlike C_{60} on this surface, the islands are all found to have the same domain orientation. Figure 2(a) shows a high-resolution image of a La@C_{82} island from which adsorption sites of the molecules on the surface may be determined and are shown in Fig. 2(b). In this model each vertex of the hexagon corresponds to a Ag trimer (bright spot on STM image) and the center of each hexagon corresponds to a Si trimer. The molecules within the hexagonally ordered island are at an angle of 30° to the Ag unit-cell vectors, parallel to the underlying $[\bar{1}10]$ Si surface lattice vectors. All molecules occupy equivalent surface sites above Ag trimers. The separation of the molecules is measured from the STM images to be $1.15 \pm 0.01 \text{ nm}$ and corresponds to three Si surface lattice constants (1.152 nm). Using Woods' notation, this reconstruction is $\text{La@C}_{82}/\text{Ag/Si}(111)-(3 \times 3)$. For coverages up to 0.5 ML, we observe molecules in only the (3×3) domain.

In order to facilitate the analysis of the domains a notation is used, as for Upward *et al.*,¹¹ based on the unreconstructed Si(111) surface. For a regular arrangement of hexagonally ordered La@C_{82} molecules with a separation of a_c , the following condition must be satisfied:

$$la_c = |m\mathbf{a} + n\mathbf{b}| = a_0 \sqrt{(m^2 + n^2 + mn)},$$

where m and n are integers, l is the integer number of molecular separations between equivalent sites on the *unreconstructed* Si(111) surface, and the vectors \mathbf{a} and \mathbf{b} , each of length a_0 (0.384 nm), are illustrated in the schematic diagram in Fig. 2(b) [note that \mathbf{a} and \mathbf{b} are not the lattice vectors chosen by convention for Si(111)] and are at an angle of $\pm 30^\circ$ to the $[11\bar{2}]$ direction.

The misorientation angle between the principal axis of the domain and the $[11\bar{2}]$ direction of the Si(111) surface is given by

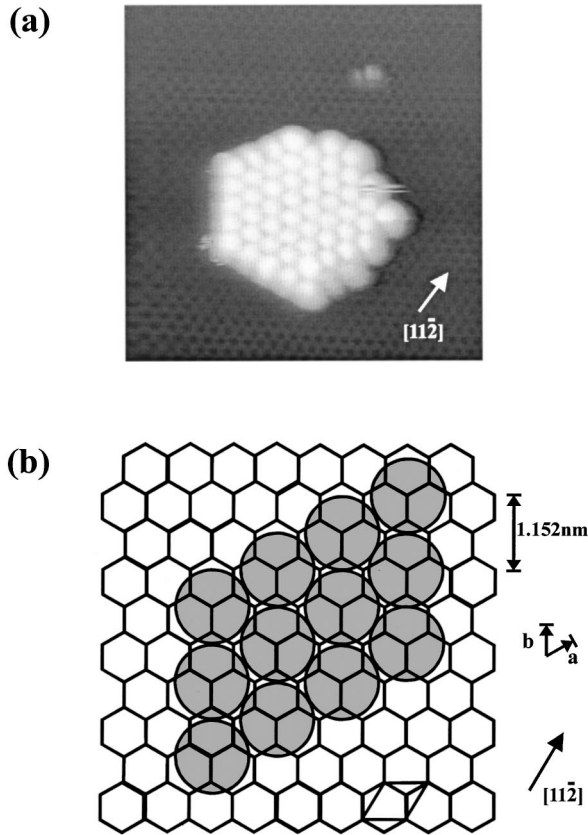


FIG. 2. (a) STM image showing a La@C_{82} island nucleated around a defect on the $\text{Ag/Si}(111)-(\sqrt{3}\times\sqrt{3})R30^\circ$. The $\sqrt{3}\times\sqrt{3}$ surface reconstruction is clearly visible ($17\times 17\text{ nm}^2$). (b) Simplified schematic of the $\text{Ag/Si}(111)-(\sqrt{3}\times\sqrt{3})R30^\circ$ reconstruction and the domain type observed for coverages $< 0.7\text{ ML}$.

$$\theta = \cos^{-1} \left(\frac{(m+n)\sqrt{3}}{2\sqrt{(m^2+n^2+mn)}} \right).$$

The principal domain therefore has the configuration $l=1$, $m=3$, $n=0$ ($\{1,3,0\}$) with an angle of 30° . Other domain configurations can be predicted for different values of n , m , and l and a small variation of the intermolecular separation a_c . Generally an equivalent domain oriented at $-\theta$ would be expected, leading to growth of at least two domains on the surface, and would preclude epitaxial growth since islands nucleated at different parts of the surface would have different orientation. In this case polycrystalline growth would be expected. However, for the special case $\theta=30^\circ$ (and also $\theta=0^\circ$), which corresponds to a commensurability between the intermolecular spacing and the silicon surface, the domains at $\pm\theta$ are indistinguishable, resulting in domains with a single orientation as observed in Fig. 2, raising the possibility of epitaxial growth.

Note that the surface phases which are observed for C_{60} on $\text{Ag/Si}(111)-(\sqrt{3}\times\sqrt{3})R30^\circ$ are not observed for La@C_{82} since the intermolecular spacing for C_{60} is different, and therefore the set of integers l , m , and n which satisfy the commensurability condition for C_{60} are different. For the case of C_{60} , $\theta=10.9^\circ$,^{11,21,22} so that double domain, poly-

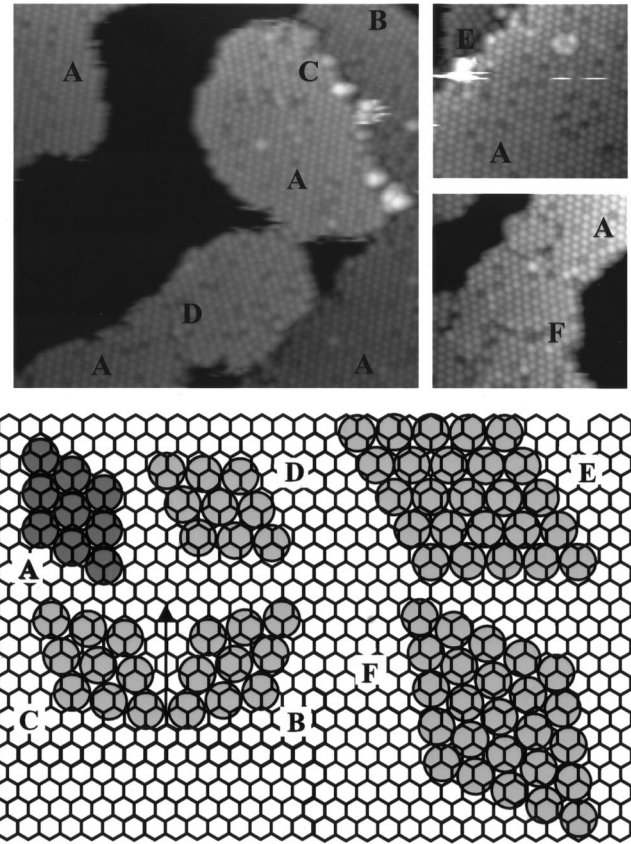


FIG. 3. STM images and schematic diagram showing the different domains observed at 0.7 ML coverage of La@C_{82} on $\text{Ag/Si}(111)-(\sqrt{3}\times\sqrt{3})R30^\circ$.

crystalline growth occurs. Note also that the relationship between commensurability and orientational order has been discussed for metal surfaces.^{8,12}

The STM images in Fig. 3 show a 0.7 monolayer coverage of La@C_{82} on the surface. At this coverage various domain orientations are observed. By studying over 100 domains it is possible to identify six different domain configurations ($A-F$). The schematic diagram in Fig. 3 shows the various observed domain configurations and these results, together with the relevant Woods notation, are summarized in Table I.

As with the lower coverage of La@C_{82} , the principal domain (A) is the most abundant and these domains are significantly larger than the other domains. Two equivalent domains (B and C) are formed with misorientation angles of 14° and -14° as discussed above. Equivalent adsorption sites are separated by two molecules ($l=2$). Fifty-six percent of molecules within these domains are adsorbed on sites that are not centered above the Ag trimers, the adsorption site for domain A . The intermolecular separation is significantly larger than the bulk separation [1.12 nm (Ref. 18)] and the intermolecular separation for the principal domain. As a result, these domains are less abundant and significantly smaller than the principal domain.

Domain D has a misorientation angle of -5° . The nearest equivalent site with respect to the $\text{Si}(111)$ lattice is two mo-

TABLE I. Measured and calculated data for the observed domains of La@C₈₂ on Ag/Si(111)-(√3 × √3)R30°.

Domain Type	A	B	C	D	E	F
Abundance (% of total domains observed at 0.7 ML)	86%	3%	3%	6%	1%	1%
Approximate area of individual domain/nm ² (at 0.7 ML)	450	90	80	130	50	100
Molecular separation within domain/nm	1.15 ± 0.01(*)	1.20 ± 0.02	1.20 ± 0.02	1.15 ± 0.02	1.15 ± 0.02	1.16 ± 0.03
Domain angle θ	30° ± 1°	14 ± 1°	-14 ± 1°	-5 ± 1°	-1 ± 1°	22 ± 1°
Domain configuration {l,m,n}	{1,3,0}	{2,5,2}	{2,2,5}	{2,3,4}	{4,7,7}	{4,2,11}
Woods notation	3 × 3	√39 × √39 R-16.1°	√39 × √37 R16.1°	2√37 × 2√37 R25.3°	7√3 × 7√3 R30°	7√3 × 7√3 R-8.2°
Calculated molecular separation/nm	1.152	1.199	1.199	1.167	1.164	1.164
Calculated domain angle θ	30°	13.9°	-13.9°	-4.7°	0°	21.8°

lecular spacings ($l=2$). However, it can be seen from the schematic that these are not equivalent sites with respect to the Ag reconstruction. For truly equivalent sites, with respect to both the Ag and Si, the domain configuration would be {6,9,12}. Although not observed in the STM images, a domain equivalent to D is expected to exist on this surface as discussed above.

Domain E has a misorientation angle of 0°. This domain, similarly to the principal domain, has a single orientation. There are equivalent adsorption sites at four molecular spacings ($l=4$). Domain F is found at a misorientation angle of -22° and also exists in low abundance. The equivalent domain with misorientation angle +22° is not observed in the STM images.

These results suggest that the domain A is the most energetically stable configuration. However, the molecular separation within this domain is still greater than the van der Waal's separation for La@C₈₂. This is likely to cause tensile strain between molecules. Nakayama *et al.*²¹ found that in strained C₆₀ domains on Ag/Si(111)-(√3 × √3)R30° missing molecule defects were observed. This is also found for the La@C₈₂ domains and can be seen in the STM images in Fig. 3.

Although several domains coexist following adsorption at higher coverage, domains $B-F$ are not stable to annealing. Figure 4 shows the effect of annealing the surface shown in Fig. 3 at ~300 °C for 3 min. The second-layer molecules have been desorbed, and only the first layer remains on the surface. Closer examination of the ordering within the first layer reveals that only the principal domain (A) remains on

the surface after annealing [Fig. 4(b)]. The result confirms that the principal domain is the most energetically stable.

B. La@C₈₂: Growth from out-of-phase domain boundaries

During the conversion from Si(111)-7 × 7 to Ag/Si(111)-(√3 × √3)R30°, nucleation occurs at different sites on the surface and areas of the reconstructed phase then grow and eventually meet. There are three equivalent registries of the reconstruction relative to the bulk Si, and at the boundaries where inequivalent domains meet, defects are observed. For growth of Ag/Si(111)-(√3 × √3)R30° at high temperature, these boundaries, known as out-of-phase boundaries, are aligned along the [112̄] directions.²³⁻²⁵ This is shown schematically in Fig. 5(a). It can be seen that the Si

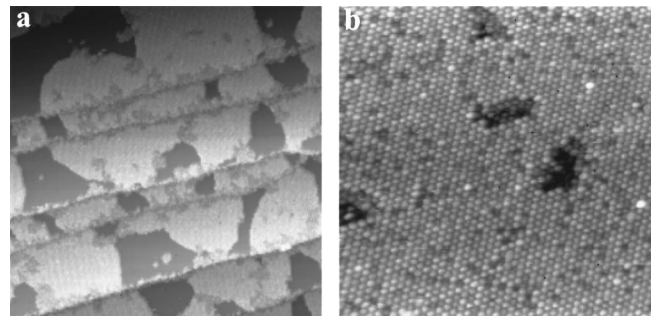


FIG. 4. STM images showing the effect of annealing a 0.7 ML coverage of La@C₈₂ on Ag/Si(111)-(√3 × √3)R30° at 300 °C. (a) 250 × 250 nm² and (b) 55 × 55 nm² (-1.5 V, 0.1 nA).

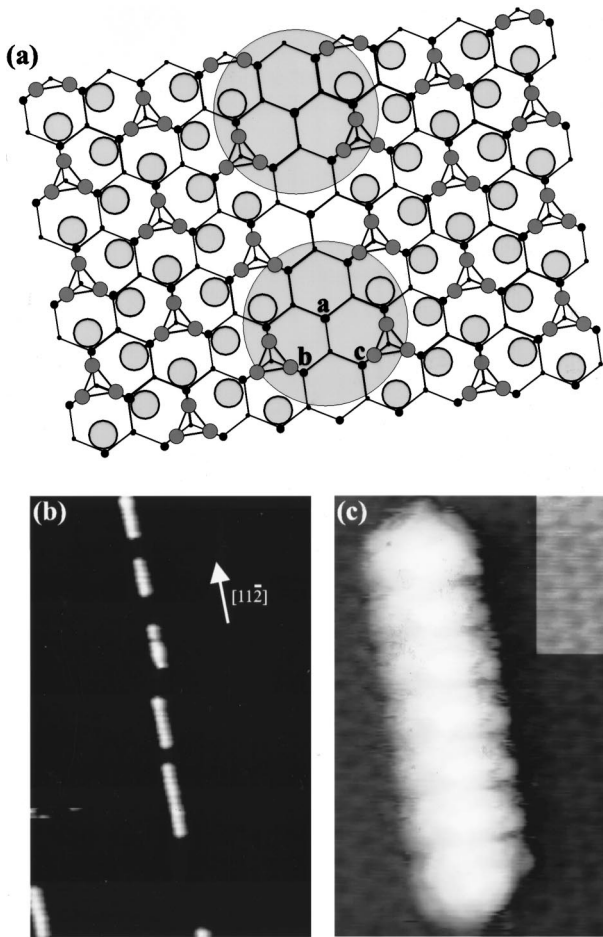


FIG. 5. (a) Schematic diagram showing an out-of-phase domain boundary (OPB). (b),(c) STM images showing adsorption of La@C_{82} molecules along the OPB (-2.8 V, 0.1 nA). (b) 80×50 nm² and (c) 10×6 nm².

trimers on either side of the OPB's have been displaced between adjacent sites in the underlying second layer. The OPB has a width of 0.77 nm.

Figure 5(b) shows La@C_{82} molecules adsorbed along an OPB. The coverage is the same as that in Fig. 1 (0.005 ML). The molecules all have the same height of 0.7 nm and line up with a regular spacing of 1.33 ± 0.01 nm [determined from the higher-resolution image, Fig. 5(c)]. At this coverage they form long chains consisting of between 5 and 15 molecules. The periodicity of the STM features associated with dangling bonds along the OPB is 0.665 nm and the La@C_{82} molecules within the chains are positioned at twice this distance (1.33 nm). By examining the higher-resolution image [Fig. 5(c)], the adsorption sites of the molecules can be identified. The molecules are centered above the first-layer atom within the center of the boundary [marked *a* in Fig. 5(a)].

It is clear that molecules adsorb preferentially on the OPB's as compared with step edges as shown in Fig. 6. In this image an OPB runs across the image and is almost completely saturated with molecules. In comparison, the step edges are less populated. The preferential adsorption is probably due to the interaction of each molecule with three Si atoms which would otherwise be bonded to a Si trimer atom

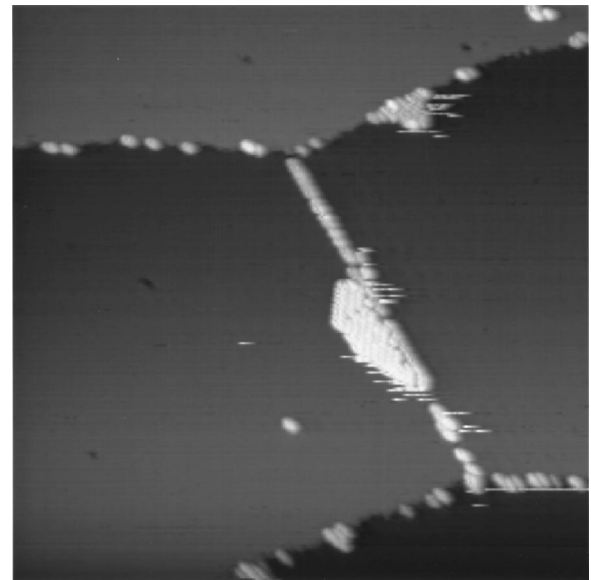


FIG. 6. STM image showing the adsorption of La@C_{82} molecules along an OPB at 0.04 ML coverage (80×80 nm²).

[marked *a* in Fig. 5(a)] or a Ag atom [marked *b* and *c* in Fig. 5(a)]. Note that steric factors inhibit the passivation of these bonds by excess Ag, which may be present on the surface, although this is possible for the dangling bonds at step edges. This factor together with the possibility of interaction with a larger number of Si atoms in the OPB adsorption sites as compared with step edges accounts for preferential adsorption at OPB's.

The formation of one-dimensional arrays of molecules is suggestive of ordering induced by intermolecular interactions. However, this would be surprising, as the molecular separation of 1.33 nm is 19% larger than the van der Waal's separation of the La@C_{82} molecules.¹⁸ Furthermore, it has

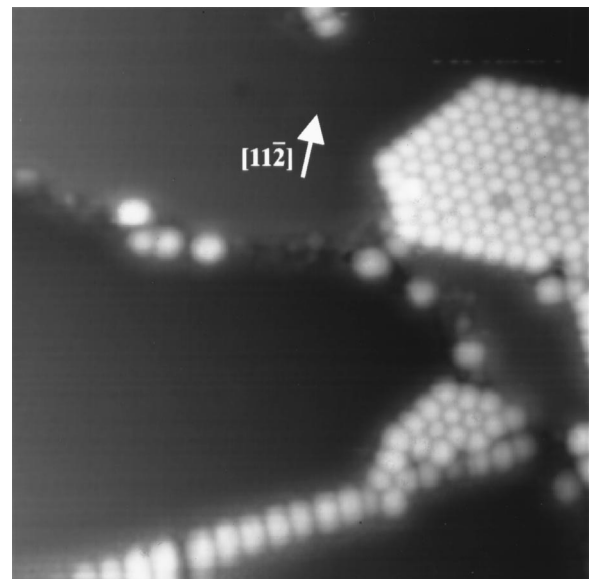


FIG. 7. STM image showing a 0.2 ML coverage of C_{84} molecules on the $\text{Ag/Si}(111)-(\sqrt{3} \times \sqrt{3})R30^\circ$ surface (30×30 nm², -2 V, 0.75 nA).

recently been found that C_{60} (Ref. 26) and, as will be shown, C_{84} also form such one-dimensional structures along these boundaries. Molecules in these arrays adopt the minimum separation and therefore the maximum packing, which is consistent with adsorption above atoms equivalent to that marked *a* in Fig. 5(a). Thus the regularity is controlled by molecule-substrate interactions, while the close-packed nature of the arrays indicates that molecules have sufficient mobility to diffuse along the OPB following adsorption.

The growth of islands starts initially from the OPB's, showing that these are the most preferential adsorption sites. This is shown in Fig. 6. The island extending from the OPB has 45 molecules within it which are ~ 0.2 nm higher than the molecules bound along the OPB. The white streaks on the image show that, unlike the molecules along the OPB, some of the molecules within the island are interacting with the tip.

C. C_{84}

A similar study was performed over a more restricted range of coverages for C_{84} . All the results discussed above for $La@C_{82}$ apply also to C_{84} . This is illustrated in Fig. 7, which shows an STM image following 0.2 ML coverage (40

h deposition) of C_{84} on $Ag/Si(111)-(\sqrt{3}\times\sqrt{3})R30^\circ$. At this coverage the only observed domain orientation is the same as domain *A* for $La@C_{82}$, with the molecules separated by 1.15 nm. Also observed in Fig. 7 are ordered rows of C_{84} molecules arranged along an OPB and a number of isolated molecules adsorbed at step edges and at defects on terrace steps.

IV. SUMMARY

We have shown that fullerene growth with orientational order is observed for adsorbate-substrate combinations in which the intermolecular spacing and the Si surface lattice constant are commensurate. This observation raises the possibility of epitaxial growth of fullerenes, and furthermore our demonstration that this mode of growth is possible for more than one fullerene species indicates that the growth of lattice matched fullerene heterostructures may be possible.

ACKNOWLEDGMENTS

This work was supported under the EC Framework V initiative within Project No. IST-1999-11617 (QIPD-DF). T.J.S.D. thanks the Royal Society for financial support.

-
- ¹For a general review, see M. S. Dresselhaus, G. Dresselhaus, and P. C. Eklund, *Science of Fullerenes and Carbon Nanotubes* (Academic, London, 1996).
- ²Y. Z. Li, J. C. Patrin, M. Chander, J. H. Weaver, L. P. F. Chibante, and R. E. Smalley, *Science* **252**, 547 (1991).
- ³R. J. Wilson, G. Meijer, D. S. Bethune, R. D. Johnson, D. D. Chambliss, M. S. de Vries, H. E. Hunziker, and H. R. Wendt, *Nature (London)* **348**, 621 (1990).
- ⁴E. I. Altman and R. J. Colton, *Phys. Rev. B* **48**, 18 244 (1993).
- ⁵J. K. Gimzewski, S. Modesti, T. David, and R. R. Schlittler, *J. Vac. Sci. Technol. B* **12**, 1942 (1994).
- ⁶Y. Z. Li, J. C. Patrin, M. Chander, J. H. Weaver, L. P. F. Chibante, and R. E. Smalley, *Phys. Rev. B* **45**, 13 837 (1992).
- ⁷X. D. Wang, T. Hashizume, H. Shinohara, Y. Saito, Y. Nishina, and T. Sakurai, *Jpn. J. Appl. Phys., Part 2* **31**, L983 (1992).
- ⁸T. Hashizume, K. Motai, X. D. Wang, R. A. Shinohara, Y. Saito, Y. Maruyama, K. Ohno, Y. Kawazoe, Y. Nishina, H. W. Pickering, Y. Kuk, and T. Sakurai, *Phys. Rev. Lett.* **71**, 2959 (1993).
- ⁹X. D. Wang, T. Hashizume, H. Shinohara, Y. Saito, Y. Nishina, and T. Sakurai, *Phys. Rev. B* **47**, 15 923 (1993).
- ¹⁰H. Xu, D. M. Chen, and W. N. Creager, *Phys. Rev. Lett.* **70**, 1850 (1993).
- ¹¹M. D. Upward, P. Moriarty, and P. H. Beton, *Phys. Rev. B* **56**, R1704 (1997).
- ¹²X.-D. Wang, S. Yamazaki, T. Hashizume, H. Shinohara, and T. Sakurai, *Phys. Rev. B* **52**, 2098 (1995).
- ¹³W. Krätschmer, L. D. Lamb, K. Fostirpoulos, and D. R. Huffman, *Nature (London)* **347**, 354 (1990).
- ¹⁴L. Dunsch, F. Ziegls, J. Fröhner, U. Kirbach, K. Klostermann, A. Bartl, and U. Feist, *Springer Series in Solid State Sciences* Vol. 117 (Springer, Berlin, 1993), pp. 39–43.
- ¹⁵T. J. S. Dennis, T. Kai, T. Tomiyama, H. Shinohara, Y. Kobayashi, H. Ishiwatari, Y. Miyake, K. Kikuchi, and Y. Achiba, *J. Phys. Chem. A* **103**, 8747 (1999); T. J. S. Dennis, S. Margadonna, K. Prassides, M. Hulman, and H. Kuzmany, *Electronic Properties of Novel Materials—Science and Technology of Molecular Nanostructures*, AIP Conference Proceedings 486, edited by H. Kuzmany, J. Fink, M. Mehring, and S. Roth, p. 187.
- ¹⁶Y. Hasegawa, Y. Ling, S. Yamazaki, T. Hashizume, H. Shinohara, A. Sakai, H. W. Pickering, and T. Sakurai, *Phys. Rev. B* **56**, 6470 (1997).
- ¹⁷N. Lin, H. Huang, S. Yang, and N. Cue, *Phys. Rev. B* **58**, 2126 (1998).
- ¹⁸T. Watanuki, A. Fujiwara, K. Ishii, Y. Matsuoka, H. Suematsu, K. Ohwada, H. Nakao, Y. Fujii, T. Kodama, K. Kikuchi, and Y. Achiba, *Electronic Properties of Novel Materials—Science and Technology of Molecular Nanostructures*, AIP Conference Proceedings 486, edited by H. Kuzmany, J. Fink, M. Mehring, and S. Roth, p. 124.
- ¹⁹W. Andreoni and A. Curioni, *Phys. Rev. Lett.* **77**, 834 (1996).
- ²⁰T. Takahashi, S. Nakatani, N. Okamoto, T. Ichikawa, and S. Kikuta, *Surf. Sci.* **242**, 54 (1991).
- ²¹T. Nakayama, J. Onoe, K. Takeuchi, and M. Aono, *Phys. Rev. B* **59**, 12 627 (1999).
- ²²K. Tsuchie, T. Nagao, and S. Hasegawa, *Phys. Rev. B* **60**, 11 131 (1999).
- ²³K. J. Wan, X. F. Lin, and J. Nogami, *Phys. Rev. B* **47**, 13 700 (1993).
- ²⁴D. W. McComb, R. A. Wolkow, and P. A. Hackett, *Phys. Rev. B* **50**, 18 268 (1994).
- ²⁵T. Nakayama, S. Watanabe, and M. Aono, *Surf. Sci.* **344**, 143 (1995).
- ²⁶T. Nakayama (personal communication).